

## Two- and Four-Electron Alkyne Ligands in Osmium–Cyclopentadienyl Chemistry: Consequences of the $\pi_{\perp} \rightarrow M$ Interaction

Jorge J. Carbó,<sup>†</sup> Pascale Crochet,<sup>‡</sup> Miguel A. Esteruelas,<sup>\*,‡</sup> Yves Jean,<sup>\*,§</sup> Agustí Lledós,<sup>\*,†</sup> Ana M. López,<sup>‡</sup> and Enrique Oñate<sup>‡</sup>

Departament de Química, Universitat Autònoma de Barcelona, 08193 Bellaterra, Barcelona, Spain, Departamento de Química Inorgánica, Instituto de Ciencia de Materiales de Aragón-Consejo Superior de Investigaciones Científicas, 50009 Zaragoza, Spain, and Laboratoire de Chimie Physique, UMR 8000, Bâtiment 490, Université de Paris-Sud, 91405 Orsay Cedex, France

Received July 19, 2001

The complexes  $\text{Os}(\eta^5\text{-C}_5\text{H}_5)\text{Cl}\{\eta^2\text{-HC}\equiv\text{CC}(\text{OH})\text{R}_2\}(\text{P}^i\text{Pr}_3)$  ( $\text{R} = \text{Ph}$  (**1a**),  $\text{Me}$  (**1b**)) react with  $\text{TlPF}_6$  to give  $[\text{Os}(\eta^5\text{-C}_5\text{H}_5)\{\eta^2\text{-HC}\equiv\text{CC}(\text{OH})\text{R}_2\}(\text{P}^i\text{Pr}_3)]\text{PF}_6$  ( $\text{R} = \text{Ph}$  (**2a**),  $\text{Me}$  (**2b**)). The structures of **1a** and **2a** have been determined by X-ray diffraction. The comparative study of the data reveals a shortening of the  $\text{Os}-\text{C}(\text{alkyne})$  distances on going from **1a** to **2a**, whereas the acetylenic bond lengths remain almost identical. Comparison of their  $^1\text{H}$  and  $^{13}\text{C}\{^1\text{H}\}$  NMR spectra shows that the  $\text{HC}\equiv$  proton resonances and the chemical shifts of the acetylenic carbon atoms of **2a** and **2b** are substantially shifted toward lower field than are those of **1a** and **1b**. DFT calculations were carried out on  $\text{Os}(\eta^5\text{-C}_5\text{H}_5)\text{Cl}(\eta^2\text{-HC}\equiv\text{CR})(\text{PH}_3)$  ( $\text{R} = \text{H}$  (**A**),  $\text{R} = \text{CH}_3$  (**A<sup>CH3</sup>**)) and  $[\text{Os}(\eta^5\text{-C}_5\text{H}_5)(\eta^2\text{-HC}\equiv\text{CR})(\text{PH}_3)]^+$  ( $\text{R} = \text{H}$  (**B**),  $\text{R} = \text{CH}_3$  (**B<sup>CH3</sup>**)) model systems in order to study the differences in bonding nature of the two parent alkyne complexes, **1** and **2**. Calculations give geometries very close to the X-ray-determined ones, and by using the GIAO method we succeed in qualitatively reproducing the experimental  $^1\text{H}$  and  $^{13}\text{C}$  chemical shifts. Both structural and spectroscopic changes can be explained by the participation of the acetylenic second  $\pi$  orbital ( $\pi_{\perp}$ ) in the metal–alkyne bonding. As we go from **1** to **2** or from **A** to **B**, the extraction of the chloride ligand transforms the 2-electron-donor alkyne ligand to a 4-electron-donor ligand, with both the  $\pi_{\parallel}$  and the  $\pi_{\perp}$  orbitals donating to the metal and stabilizing the otherwise 16-electron unsaturated complex **2**. Calculations also predict an increase of dissociation energies of the alkyne, and an enhancement in the energy of rotation of the alkyne, for complex **B**. Finally, Bader's atoms in molecules (AIM) analysis shows that differences in coordination nature are also reflected in the topological properties of electron density.

### Introduction

The  $\pi$ -alkyne complexes are some of the most important kinds of transition-metal compounds. They are intermediate species in terminal alkyne to vinylidene rearrangements<sup>1</sup> and in homogeneous and heterogeneous catalytic reactions, including hydrogenation,<sup>2</sup>

hydrosilylation,<sup>3</sup> oligomerization,<sup>4</sup> polymerization,<sup>5</sup> metathesis,<sup>6</sup> condensation of terminal alkynes with several organic molecules (allyl alcohols,<sup>7</sup>  $\alpha,\beta$ -unsaturated ketones,<sup>8</sup> alkenes,<sup>9</sup> dienes,<sup>10</sup> and alkynes<sup>11</sup>), cycloisomerization of 1,6-enynes,<sup>12</sup> and hydroamination.<sup>13</sup> In addi-

<sup>†</sup> Universitat Autònoma de Barcelona.

<sup>‡</sup> Instituto de Ciencia de Materiales de Aragón-Consejo Superior de Investigaciones Científicas.

<sup>§</sup> Université de Paris-Sud.

(1) (a) Silvestre, J.; Hoffman, R. *Helv. Chim. Acta* **1985**, *68*, 1461. (b) Lomprey, J. R.; Selegue, J. P. *J. Am. Chem. Soc.* **1992**, *114*, 5518. (c) Wakatsuki, Y.; Koga, N.; Yamazaki, H.; Morokuma, K. *J. Am. Chem. Soc.* **1994**, *116*, 8105. (d) de los Ríos, I.; Jiménez-Tenorio, M.; Puerta, M. C.; Valerga, P. *J. Chem. Soc., Chem. Commun.* **1995**, 1757. (e) Wakatsuki, Y.; Koga, N.; Werner, H.; Morokuma, K. *J. Am. Chem. Soc.* **1997**, *119*, 360. (f) de los Ríos, I.; Jiménez-Tenorio, M.; Puerta, M. C.; Valerga, P. *J. Am. Chem. Soc.* **1997**, *119*, 6529. (g) Bustelo, E.; Jiménez-Tenorio, M.; Puerta, M. C.; Valerga, P. *Organometallics* **1999**, *18*, 950. (h) Bustelo, E.; Jiménez-Tenorio, M.; Puerta, M. C.; Valerga, P. *Organometallics* **1999**, *18*, 4563. (i) Puerta, M. C.; Valerga, P. *Coord. Chem. Rev.* **1999**, *193–195*, 977.

(2) (a) Chaloner, P. A.; Esteruelas, M. A.; Joó, F.; Oro, L. A.; *Homogeneous Hydrogenation*; Kluwer Academic: Dordrecht, The Netherlands, 1994. (b) Esteruelas, M. A.; Oro, L. A. *Chem. Rev.* **1998**, *98*, 577.

(3) Marciniak, B.; Gulinsky, J.; Urbaniak, W.; Kornetka, Z. W. In *Comprehensive Handbook on Hydrosilylation*; Marciniak, B., Ed.; Pergamon: Oxford, U.K., 1992.

(4) Bruneau, C.; Dixneuf, P. H. *Acc. Chem. Res.* **1999**, *32*, 311.

(5) (a) Simionescu, C. I.; Percec, V. *Prog. Polym. Sci.* **1982**, *8*, 133. (b) Masuda, T.; Higashimura, T. *Acc. Chem. Res.* **1984**, *17*, 51. (c) Katz, T. J.; Haker, S. M.; Kendrick, R. D.; Yannoni, C. S. *J. Am. Chem. Soc.* **1985**, *107*, 2182. (d) Szymanska-Buzar, T.; Glowiak, T. *Polyhedron* **1998**, *17*, 3419. (e) Szymanska-Buzar, T.; Glowiak, T. *J. Organomet. Chem.* **1999**, *575*, 98. (f) Szymanska-Buzar, T.; Glowiak, T. *J. Organomet. Chem.* **1999**, *585*, 215.

(6) Schrock, R. R. *Acc. Chem. Res.* **1986**, *19*, 342.

(7) (a) Trost, B. M.; Flygare, J. A. *J. Am. Chem. Soc.* **1992**, *114*, 5476. (b) Trost, B. M.; Kulawiec, R. J. *J. Am. Chem. Soc.* **1992**, *114*, 5579. (c) Trost, B. M.; Martinez, J. A.; Kulawiec, R. J.; Indolese, A. F. *J. Am. Chem. Soc.* **1993**, *115*, 10402. (d) Trost, B. M.; Vidal, B.; Thommen, M. *Chem. Eur. J.* **1999**, *5*, 1055.

(8) Trost, B. M.; Pinkerton, A. B. *J. Am. Chem. Soc.* **1999**, *121*, 1988. (9) Trost, B. M.; Indolese, A. J. *Am. Chem. Soc.* **1993**, *115*, 8831. (10) (a) Trost, B. M.; Imi, K.; Indolese, A. F. *J. Am. Chem. Soc.* **1993**, *115*, 8831. (b) Trost, B. M. *Chem. Ber.* **1996**, *129*, 1313.

(11) Yi, C. S.; Liu, N. *Organometallics* **1998**, *17*, 3158.

(12) Trost, B. M.; Toste, D. J. *Am. Chem. Soc.* **1999**, *121*, 9728.

tion, they show applications in stoichiometric organic synthesis such as 2 + 2 + 2 cycloadditions,<sup>14</sup> quinone synthesis,<sup>15</sup> and complex condensations with carbenes.<sup>16</sup>

The broad range of applications of  $\pi$ -alkyne transition-metal complexes has also attracted the interest of theoretical chemists. Thus, several aspects of the coordination of alkynes to naked atoms,<sup>17</sup> surfaces,<sup>18</sup> and complexes<sup>19</sup> have been studied. Frenking and Fröhlich have recently reviewed these investigations.<sup>20</sup>

The chemical bonding in transition-metal alkyne complexes can be described in a way similar to that for the transition-metal alkene complexes. The bonding is considered to arise either from donor–acceptor interactions between the alkyne ligand and the transition metal or as a metallacyclic compound. A major difference between alkene and alkyne complexes is that the alkyne ligand has a second occupied  $\pi$  orbital orthogonal to the  $MC_2$  plane ( $\pi_{\perp}$ ) which, in some cases, engages in the transition-metal–alkyne bonding. In that case, the alkyne is a four-electron-donor ligand by means of its  $\pi_{\parallel}$  and  $\pi_{\perp}$  orbitals. The alkyne ligand also acts as an electron acceptor by means of its  $\pi^*$  orbitals. The  $\pi_{\perp}^*$  orbital is, however, of local  $a_2$  symmetry (within the  $C_{2v}$  group), which prevents it from significant interaction with the filled d metal orbital ( $\delta$  type interaction). The only significant interaction involves the acceptor orbital lying in the  $MC_2$  plane ( $\pi_{\parallel}^*$  of local  $b_1$  symmetry): i.e., the orbital already at work in the alkene complexes.

The chemistry of four-electron-donating alkynes has been centered at early transition metals, mainly molybdenum and tungsten.<sup>21</sup> Thus, a wide variety of six-coordinate Mo(II) and W(II) complexes with four-electron-donor alkynes have been synthesized.<sup>21,22</sup> Four-coordinated  $d^6$  complexes of the types  $ML(alkyne)_3$ <sup>23</sup> and

$ML_2(alkyne)_2$ <sup>24</sup> have been also reported. In contrast, five-coordinate  $d^6$  monoalkyne complexes with the general formula  $ML_4(alkyne)$  are very scarce,<sup>25</sup> and  $MCpL(alkyne)$  species are unknown.

Despite the high kinetic inertia of the  $OsCpL_3$  compounds,<sup>26</sup> we have reported overwhelming evidence showing that the complex  $Os(\eta^5-C_5H_5)Cl(P^iPr_3)_2$  is a labile starting material for the development of new cyclopentadienyl–osmium chemistry,<sup>27</sup> including  $Os(\eta^5-C_5H_5)Cl(\eta^2-alkyne)(P^iPr_3)$  complexes,<sup>28</sup> where the alkyne acts as a two-electron-donor ligand. We now show that these compounds can be converted into stable  $[Os(\eta^5-C_5H_5)(\eta^2-alkyne)(P^iPr_3)]^+$  species, containing a four-electron-donating alkyne.

With regard to the complexes containing two-electron-donor alkyne ligands, the donation from the  $\pi_{\perp}$  orbital disturbs the molecular structure and reactivity<sup>21,29</sup> as well as spectroscopic properties<sup>30</sup> of the  $\pi$ -alkyne complex. Despite the efforts made toward an understanding of metal–alkyne bonding,<sup>17–20</sup> quantitative theoretical studies on the two- vs four-electron dichotomy of the alkyne ligands are still lacking. The discovery of the complexes  $Os(\eta^5-C_5H_5)Cl(\eta^2-alkyne)(P^iPr_3)$  and  $[Os(\eta^5-C_5H_5)(\eta^2-alkyne)(P^iPr_3)]^+$  has prompted us to carry out theoretical calculations on the bonding scheme, geometries and bond energies, rotational barriers, and NMR properties in these unusual osmium compounds.

In this paper, we report the synthesis and spectroscopic and X-ray characterization of  $[Os(\eta^5-C_5H_5)(\eta^2-alkyne)(P^iPr_3)]^+$ , the X-ray characterization of  $Os(\eta^5-C_5H_5)Cl(\eta^2-alkyne)(P^iPr_3)$ , and the results of the theoretical study on the different bonding natures of the metal–alkyne interaction.

## Results and Discussion

**1. Synthesis and X-ray and Spectroscopic Characterization of  $Os(\eta^5-C_5H_5)Cl(\eta^2-alkyne)(P^iPr_3)$  and  $[Os(\eta^5-C_5H_5)(\eta^2-alkyne)(P^iPr_3)]^+$ .** As a consequence of the large steric hindrance experienced by the triisopropylphosphine ligands of  $Os(\eta^5-C_5H_5)Cl(P^iPr_3)_2$ , in pentane, the splitting of a phosphorus–osmium bond is favored. Thus, the addition at room temperature of 1.2 equiv of 1,1-diphenyl-2-propyn-1-ol and 2-methyl-

(13) Müller, T. E.; Beller, M. *Chem. Rev.* **1998**, *98*, 675.

(14) Vollhardt, K. P. C. *J. Org. Chem.* **1984**, *59*, 1574.

(15) Liebeskind, L. S.; Jewell, C. F., Jr. *J. Organomet. Chem.* **1985**, *285*, 305.

(16) (a) Dotz, K. H. *Angew. Chem., Int. Ed. Engl.* **1984**, *23*, 587. (b) Wulf, W. D.; Gilbertson, S. R.; Springer, J. P. *J. Am. Chem. Soc.* **1986**, *108*, 520.

(17) (a) Miralles-Sabater, J.; Merchán, M.; Nebot-Gil, I.; Viruela-Martin, P. M. *J. Phys. Chem.* **1988**, *92*, 4853. (b) Sodupe, M.; Bauschlicher, G. W. *J. Phys. Chem.* **1991**, *95*, 8640. (c) Sodupe, M.; Bauschlicher, G. W., Jr.; Langhoff, S. R.; Partridge, H. *J. Phys. Chem.* **1992**, *96*, 2118. (d) Mitchell, S. A.; Blitt, M. A.; Fournier, R. *Can. J. Chem.* **1994**, *72*, 587. (e) Böhme, M.; Wagener, T.; Frenking, G. *J. Organomet. Chem.* **1996**, *520*, 31.

(18) Sellers, H. *J. Phys. Chem.* **1990**, *94*, 8329.

(19) (a) Kitaura, K.; Sakaki, S.; Morokuma, K. *Inorg. Chem.* **1981**, *20*, 2292. (b) Ziegler, T. *Inorg. Chem.* **1985**, *24*, 1547. (c) Nielson, A. J.; Boyd, P. D. W.; Clark, G. R.; Hunt, T. A.; Metson, J. B.; Rickard, C. E. F.; Schwerdtfeger, P. *Polyhedron* **1992**, *11*, 1419. (d) Stegmann, R.; Neuhaus, A.; Frenking, G. *J. Am. Chem. Soc.* **1993**, *115*, 11930. (e) Pidun, U.; Frenking, G. *Organometallics* **1995**, *14*, 5325. (f) Li, J.; Schreckenbach, G.; Ziegler, T. *Inorg. Chem.* **1995**, *34*, 3245. (g) Pidun, U.; Frenking, G. *J. Organomet. Chem.* **1996**, *525*, 269. (h) Frenking, G.; Pidun, U. *J. Chem. Soc., Dalton Trans.* **1997**, 1653. (i) Hyla-Kryspin, I.; Koch, J.; Gleiter, R.; Klettke, T.; Walther, D. *Organometallics* **1998**, *17*, 4724. (j) Decker, S. A.; Klobukowski, M. *J. Am. Chem. Soc.* **1998**, *120*, 9342. (k) Kovács, A.; Frenking, G. *Organometallics* **1999**, *18*, 887.

(20) Frenking, G.; Fröhlich, N. *Chem. Rev.* **2000**, *100*, 717.

(21) (a) Templeton, J. L. *Adv. Organomet. Chem.* **1989**, *29*, 1. (b) Baker, P. B. *Adv. Organomet. Chem.* **1996**, *40*, 45.

(22) (a) Frohnapfel, D. S.; Reinartz, S.; White, P. S.; Templeton, J. L. *Organometallics* **1998**, *17*, 3759. (b) Frohnapfel, D. S.; Enriquez, A. E.; Templeton, J. L. *Organometallics* **2000**, *19*, 221.

(23) See for example: (a) Tate, D. P.; Augl, J. M. *J. Am. Chem. Soc.* **1963**, *85*, 2174. (b) Wink, D. J.; Creagan, T. *Organometallics* **1990**, *9*, 328. (c) Szymanska-Buzar, T.; Glowiak, T. *J. Organomet. Chem.* **1994**, *467*, 233. (d) Yeh, W.-Y.; Ting, C.-S. *Organometallics* **1995**, *14*, 1417. (e) Mealli, C.; Masi, D.; Galindo, A.; Pastor, A. *J. Organomet. Chem.* **1998**, *569*, 21.

(24) See for example: (a) Dötz, K. H.; Müklemeyer, J. *Angew. Chem., Int. Ed. Engl.* **1982**, *21*, 929. (b) Salt, J. E.; Girolami, G. J.; Wilkinson, G.; Motevolli, M.; Thornton-Pett, M.; Hurthouse, M. B. *J. Chem. Soc., Dalton Trans.* **1985**, 685. (c) Wink, D. J.; Fox, J. R.; Cooper, J. *J. Am. Chem. Soc.* **1985**, *107*, 5012.

(25) (a) Wink, D. J.; Creagan, T. *J. Am. Chem. Soc.* **1990**, *112*, 8585. (b) Ishiro, H.; Kuwata, S.; Ishii, Y.; Hidai, M. *Organometallics* **2001**, *20*, 13.

(26) Atwood, J. D. *Inorganic and Organometallic Reaction Mechanisms*; VCH: New York, 1997; Chapter 3.

(27) (a) Esteruelas, M. A.; Gómez, A. V.; López, A. M.; Oro, L. A. *Organometallics* **1996**, *15*, 878. (b) Crochet, P.; Esteruelas, M. A.; López, A. M.; Ruiz, N.; Tolosa, J. I. *Organometallics* **1998**, *17*, 3479. (c) Crochet, P.; Esteruelas, M. A.; Gutiérrez-Puebla, E. *Organometallics* **1998**, *17*, 3141. (d) Baya, M.; Crochet, P.; Esteruelas, M. A.; Gutiérrez-Puebla, E.; López, A. M.; Oñate, E.; Tolosa, J. I. *Organometallics* **2000**, *19*, 275. (e) Baya, M.; Crochet, P.; Esteruelas, M. A.; Gutiérrez-Puebla, E.; López, A. M.; Modrego, J.; Oñate, E.; Vela, N. *Organometallics* **2000**, *19*, 2585. (f) Esteruelas, M. A.; López, A. M.; Tolosa, J. I.; Vela, N. *Organometallics* **2000**, *19*, 4650. (g) Baya, M.; Crochet, P.; Esteruelas, M. A.; Oñate, E. *Organometallics* **2001**, *20*, 240.

(28) Esteruelas, M. A.; López, A. M.; Ruiz, N.; Tolosa, J. I. *Organometallics* **1997**, *16*, 4657.

(29) Frohnapfel, D. S.; Templeton, J. L. *Coord. Chem. Rev.* **2000**, *206–207*, 199.

(30) Templeton, J. L.; Ward, B. C. *J. Am. Chem. Soc.* **1980**, *102*, 3288.

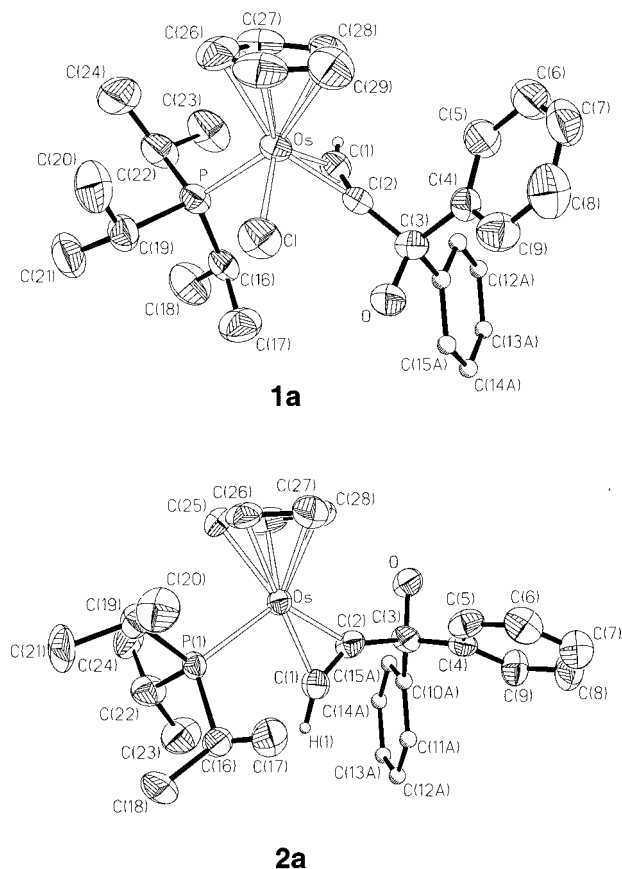
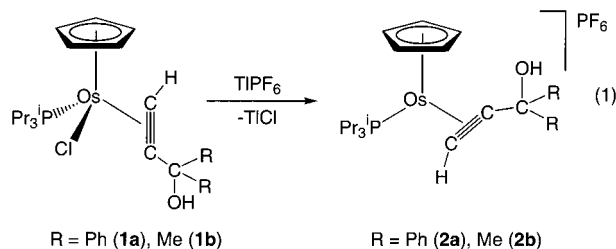


**Figure 1.** Molecular diagrams for the complex  $\text{Os}(\eta^5\text{-C}_5\text{H}_5)\text{Cl}\{\eta^2\text{-HC}\equiv\text{CC}(\text{OH})\text{Ph}_2\}(\text{P}^i\text{Pr}_3)$  (**1a**) and for the cation of  $[\text{Os}(\eta^5\text{-C}_5\text{H}_5)\{\eta^2\text{-HC}\equiv\text{CC}(\text{OH})\text{Ph}_2\}(\text{P}^i\text{Pr}_3)]\text{PF}_6$  (**2a**). Thermal ellipsoids are shown at 50% probability.

3-butyn-2-ol to pentane solutions of this complex gives rise to the formation of the  $\pi$ -alkyne derivatives  $\text{Os}(\eta^5\text{-C}_5\text{H}_5)\text{Cl}\{\eta^2\text{-HC}\equiv\text{CC}(\text{OH})\text{R}_2\}(\text{P}^i\text{Pr}_3)$  ( $\text{R} = \text{Ph}$  (**1a**),  $\text{Me}$  (**1b**)). In toluene solutions, at 85 °C, complexes **1a** and **1b** evolve into the allenylidene ( $\text{Os}(\eta^5\text{-C}_5\text{H}_5)\text{Cl}(\text{C}=\text{C}=\text{CPh}_2)(\text{P}^i\text{Pr}_3)$ )<sup>27b</sup> and alkenylvinylidene ( $\text{Os}(\eta^5\text{-C}_5\text{H}_5)\text{Cl}(\text{C}=\text{CHC}(\text{CH}_3)=\text{CH}_2)(\text{P}^i\text{Pr}_3)$ ) complexes,<sup>28</sup> respectively, with loss of a water molecule from the alkyne. Treatment at room temperature of dichloromethane solutions of **1a** and **1b** with  $\text{TlPF}_6$  produces the extraction of the chloride ligand and the formation of  $[\text{Os}(\eta^5\text{-C}_5\text{H}_5)\{\eta^2\text{-HC}\equiv\text{CC}(\text{OH})\text{R}_2\}(\text{P}^i\text{Pr}_3)]\text{PF}_6$  ( $\text{R} = \text{Ph}$  (**2a**),  $\text{Me}$  (**2b**)), which are isolated in high yield (eq 1). In contrast



to **1a** and **1b**, **2a** and **2b** are stable in solution for a long time. The dehydration of the alkynes, as well as their transformation into the corresponding allenylidene and alkenylvinylidene species, is not observed.

Figure 1 shows the X-ray structures of **1a** and **2a**, whereas selected bond distances and angles for both compounds are listed in Table 1.

The geometry around the osmium atom of **1a** can be described as a three-legged piano stool. The angles  $\text{P}-\text{Os}-\text{Cl}$ ,  $\text{P}-\text{Os}-\text{M}(2)$  ( $\text{M}(2)$  is the midpoint of the carbon–carbon triple bond of the alkyne), and  $\text{Cl}-\text{Os}-\text{M}(2)$  are 86.85(6), 86.73(18), and 103.8(2)°, respectively.

The carbon–carbon triple bond ( $\text{C}(1)-\text{C}(2)$ ) forms an angle of 28° with the  $\text{Os}-\text{Cl}$  bond. The torsion angle  $\text{Cl}-\text{Os}-\text{C}(1)-\text{C}(2)$  is 156.3°, whereas the torsion angle  $\text{P}-\text{Os}-\text{C}(1)-\text{C}(2)$  is 112°. As expected, the coordination of the alkyne to the metal has a slight effect on the acetylenic bond length. Thus, the  $\text{C}(1)-\text{C}(2)$  distance (1.222(8) Å) is about 0.04 Å longer than the average value in free alkynes (1.18 Å).<sup>31</sup> The  $\text{Os}-\text{C}(1)$  (2.142(7) Å) and  $\text{Os}-\text{C}(2)$  (2.163(6) Å) bond lengths are statistically identical. In addition, it should be mentioned that the substituted carbon atom of the alkyne ( $\text{C}(2)$ ) is pointed away from the bulky triisopropylphosphine ligand. Although two isomers of **1a** could be formed in the solid state, this indicates that only one of them is obtained, the isomer with less steric hindrance.

The geometry around the osmium atom of **2a** can be rationalized as a two-legged piano stool with the acetylenic  $\text{C}(1)-\text{C}(2)$  bond and the  $\text{Os}-\text{P}$  axis in the same plane. The  $\text{P}-\text{Os}-\text{C}(1)-\text{C}(2)$  torsion angle is 183.7°. Interestingly, although the  $\text{C}(1)-\text{C}(2)$  bond lengths in **2a** (1.26(2) Å) and **1a** are very similar, there are substantial differences between the respective  $\text{Os}-\text{C}$  distances of both compounds. The  $\text{Os}-\text{C}(1)$  distance in **2a** (1.992(9) Å) is about 0.15 Å shorter than the related parameter in **1a**, whereas the  $\text{Os}-\text{C}(2)$  bond length in **2a** (1.981(8) Å) is about 0.18 Å shorter than that in **1a**. As in **1a**, the substituted  $\text{C}(2)$  carbon atom of **2a** is pointed away from the phosphine ligand.

There are also substantial differences between the  $^1\text{H}$ ,  $^{13}\text{C}\{^1\text{H}\}$ , and  $^{31}\text{P}\{^1\text{H}\}$  NMR spectra for complexes of types **1** and **2**. In the  $^1\text{H}$  NMR spectra of **1a** and **1b** the  $\text{HC}\equiv$  resonances of the alkynes appear at 4.3 and 3.73 ppm, respectively, as doublets with  $\text{H}-\text{P}$  coupling constants of about 9 Hz. The same  $\text{HC}\equiv$  resonances for complexes **2a** and **2b** appear also as doublets, but at lower field (about 9.3 ppm) and with  $\text{H}-\text{P}$  coupling constants (26.4 Hz for both compounds) much higher than those found in **1a** and **1b**. A similar relationship is observed in the  $^{13}\text{C}\{^1\text{H}\}$  NMR spectra. In the  $^{13}\text{C}\{^1\text{H}\}$  NMR spectra of **1a** and **1b**, the resonances corresponding to the acetylenic carbon atoms appear at 82.2 and 69.1 ppm ( $\equiv\text{CR}$ ) and at 57.5<sup>32</sup> and 49.6 ppm ( $\text{HC}\equiv$ ), while in the spectra of **2a** and **2b** they are observed at 179.0 and 182.8 ppm ( $\equiv\text{CR}$ ) and at 146.0 and 143.3 ppm ( $\text{HC}\equiv$ ): i.e., shifted about 100 ppm toward low field. The  $^{31}\text{P}\{^1\text{H}\}$  NMR spectra also indicate that the electronic properties of osmium atoms in compounds of types **1** and **2** are different. While the chemical shifts of the singlets of **1a** and **1b** are 10.0 and 9.5 ppm, respectively, those of **2a** and **2b** are 38.0 and 36.3 ppm. These differences indicate that the alkyne ligand of **1a** and **1b** acts as a two-electron-donor ligand, while in **2a** and **2b** it acts as a four-electron-donor ligand.<sup>30</sup>

## 2. Computational Studies on the Alkyne Complexes.

The differences in the alkyne–osmium bonding

(31) Allen, F. H.; Kennard, O.; Watson, D. G.; Brammer, L.; Orpen, A. G.; Taylor, R. *J. Chem. Soc., Perkin Trans.* **1987**, S1.

(32) This chemical shift was erroneously reported as 122.9 ppm in ref 27b.



**Table 1. Selected Bond Distances (Å) and Angles (deg) for the Complexes  $\text{Os}(\eta^5\text{-C}_5\text{H}_5)\text{Cl}\{\eta^2\text{-HC}\equiv\text{CC}(\text{OH})\text{Ph}_2\}(\text{P}^i\text{Pr}_3)$  (**1a**) and  $[\text{Os}(\eta^5\text{-C}_5\text{H}_5)\{\eta^2\text{-HC}\equiv\text{CC}(\text{OH})\text{Ph}_2\}(\text{P}^i\text{Pr}_3)]\text{PF}_6$  (**2a**).**

	<b>1a</b>	<b>2a</b>	<b>1a</b>	<b>2a</b>
Os–Cl	2.4445(16)		Os–C(27)	2.190(7)
Os–P	2.3444(17)	2.410(2)	Os–C(28)	2.203(7)
Os–C(1)	2.142(7)	1.992(9)	Os–C(29)	2.246(7)
Os–C(2)	2.163(6)	1.981(8)	C(1)–C(2)	1.222(8)
Os–C(25)	2.237(6)	2.222(7)	C(2)–C(3)	1.499(9)
Os–C(26)	2.246(7)	2.220(9)		
Cl–Os–P	86.85(6)		Os–C(1)–C(2)	74.4(4)
Cl–Os–M(1) <sup>a</sup>	115.5(3)		Os–C(1)–H(1)	125(5)
Cl–Os–M(2) <sup>a</sup>	103.8(2)		Os–C(2)–C(1)	72.6(5)
P–Os–M(1)	129.6(2)	119.2(4)	Os–C(2)–C(3)	137.8(5)
P–Os–M(2)	86.73(18)	99.2(4)	H(1)–C(1)–C(2)	154(5)
M(1)–Os–M(2)	121.0(3)	141.7(4)	C(1)–C(2)–C(3)	148.8(7)
				145(4)
				140.3(9)

<sup>a</sup> M(1) and M(2) are the midpoints of the C(25)–C(29) Cp and C(1)–C(2) acetylenic ligands.

in compounds **1** and **2** has been studied by means of DFT calculations (B3LYP functional), in conjunction with Bader's atoms in molecules (AIM) theory. The study has been performed using  $\text{Os}(\eta^5\text{-C}_5\text{H}_5)\text{Cl}(\eta^2\text{-HC}\equiv\text{CH})(\text{PH}_3)$  (**A**) and  $[\text{Os}(\eta^5\text{-C}_5\text{H}_5)(\eta^2\text{-HC}\equiv\text{CH})(\text{PH}_3)]^+$  (**B**) as model systems of complexes of types **1** and **2**, respectively. Additionally, we have also considered  $\text{Os}(\eta^5\text{-C}_5\text{H}_5)\text{Cl}(\eta^2\text{-HC}\equiv\text{CCH}_3)(\text{PH}_3)$  (**A<sup>CH3</sup>**) and  $[\text{Os}(\eta^5\text{-C}_5\text{H}_5)(\eta^2\text{-HC}\equiv\text{CCH}_3)(\text{PH}_3)]^+$  (**B<sup>CH3</sup>**) in order to model the substituted alkynes.

**Bonding Scheme.** The way the alkyne ligand binds the metal center in complexes **A** and **B** can be analyzed first by using a fragment MO analysis.<sup>33</sup> In the former, the alkyne interacts with a 16-electron metal fragment of  $d^6\text{-}[\text{Os}(\eta^5\text{-C}_5\text{H}_5)\text{LL}']$  type. Schilling et al. have shown that, in such complexes, only the  $\pi_{||}$  orbital of the alkyne interacts with a vacant d orbital on the metal center,<sup>34</sup> this 2-electron-donor behavior leading to an 18-electron alkyne complex. A back-donation interaction, involving  $\pi_{||}^*$ , is also at work and was found to be responsible for the orientation of the alkyne with respect to the metal fragment. Complex **B** can be described as a 14-electron fragment of  $d^6\text{-}[\text{Os}(\eta^5\text{-C}_5\text{H}_5)\text{L}]^+$  type interacting with an alkyne ligand in a geometry where the P, Os, C1, and C2 atoms are coplanar. There are now two vacant d orbitals on the metal fragment, one symmetrical and one antisymmetrical with respect to the molecular symmetry plane. The symmetry properties of these two empty d orbitals match those of the occupied  $\pi_{||}$  and  $\pi_{\perp}$  orbitals (Figure 2a,b) so that the alkyne acts as a 4-electron-donor ligand, leading to an 18-electron complex. Note that a further stabilization results from the back-donation interaction which involves the  $\pi_{||}^*$  orbital (Figure 2c). Similar orbital interaction schemes have been derived by Hoffmann and co-workers for  $d^4$  molybdenum systems<sup>35</sup> and, more recently, by Decker and Klobukowski for the  $\text{M}(\text{CO})_3(\text{C}_2\text{H}_2)$  complexes (M = Fe, Ru).<sup>19j</sup> In each case, the participation of both the  $\pi_{||}$  and  $\pi_{\perp}$  orbitals in donating electrons to the metal allows the complex to reach the 18-electron count. This qualitative analysis, derived from the DFT-computed molecular orbitals, is further supported by NBO (natural bonding orbitals) population analysis carried out on complexes

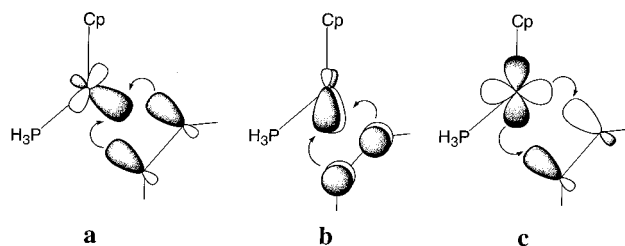


**Figure 2.** Schematic representation of the donative (a and b) and back-donative (c) interactions for metal–alkyne bonding in the complex  $[\text{Os}(\eta^5\text{-C}_5\text{H}_5)(\eta^2\text{-HC}\equiv\text{CH})(\text{PH}_3)]^+$  (**B**).

**A** and **B**. The population of the alkyne  $\pi_{\perp}$  NBO orbital is significantly lower in **B** (1.679e) than in **A** (1.982e), showing that  $\pi_{\perp}$  is involved in the alkyne–metal bonding in **B** but not in **A**. Note that, in both complexes, the participation of  $\pi_{\perp}^*$  is almost negligible, the NBO populations being equal to 0.017e and 0.042 e in **A** and **B**, respectively.

This qualitative analysis shows that the alkyne ligand acts as a two- and a four-electron donor in complexes **A** and **B**, respectively. Therefore, these two parent complexes provide the opportunity to study how the geometrical, electronic, and energetic properties of an alkyne complex depend on the donor behavior of that ligand.

**Geometries and Bond Energies.** The computed optimized geometries of complexes  $\text{Os}(\eta^5\text{-C}_5\text{H}_5)\text{Cl}(\eta^2\text{-HC}\equiv\text{CR})(\text{PH}_3)$  (R = H (**A**),  $\text{CH}_3$  (**A<sup>CH3</sup>**)) and  $[\text{Os}(\eta^5\text{-C}_5\text{H}_5)(\eta^2\text{-HC}\equiv\text{CR})(\text{PH}_3)]^+$  (R = H (**B**),  $\text{CH}_3$  (**B<sup>CH3</sup>**)) are presented in Figure 3. In **A**, the  $\text{C}\equiv\text{C}$  acetylene bond forms an angle of about  $25^\circ$  with the Os–Cl bond. The computed torsion angle between P–Os–C1–C2 atoms is  $106.0^\circ$  for complex **A**, while for **B** it is  $179.9^\circ$ , indicating that acetylenic carbon, osmium, and phosphorus atoms are almost coplanar in complex **B**. These results agree with the alkyne conformations of the X-ray-determined structures. The differences in conformational preferences of the two complexes will be commented upon later. In the case of substituted alkynes (R =  $\text{CH}_3$ ), two different isomers have been considered for each complex (**A<sup>CH3</sup>** and **B<sup>CH3</sup>**), depending on which acetylenic carbon is substituted. Thus, the methyl substituent can lie in the phosphine ligand side (endo) or in the opposite side (exo). The endo isomers (**An<sup>CH3</sup>** and **Bn<sup>CH3</sup>**) are 0.8 and 2.8 kcal mol<sup>-1</sup> higher in energy than their respective exo forms (**Ax<sup>CH3</sup>** and **Bx<sup>CH3</sup>**) for complexes **A<sup>CH3</sup>** and **B<sup>CH3</sup>**, respectively. This

(33) Albright, T. A.; Burdett, J. K.; Whangbo, M. H. *Orbital Interactions in Chemistry*; Wiley: New York, 1985.

(34) (a) Schilling, B. E. R.; Hoffmann, R.; Faller, J. W. *J. Am. Chem. Soc.* **1979**, *101*, 585. (b) Schilling, B. E. R.; Hoffmann, R.; Faller, J. W. *J. Am. Chem. Soc.* **1979**, *101*, 592.

(35) Tatsumi, K.; Hoffmann, R.; Templeton, J. L. *Inorg. Chem.* **1982**, *21*, 466.

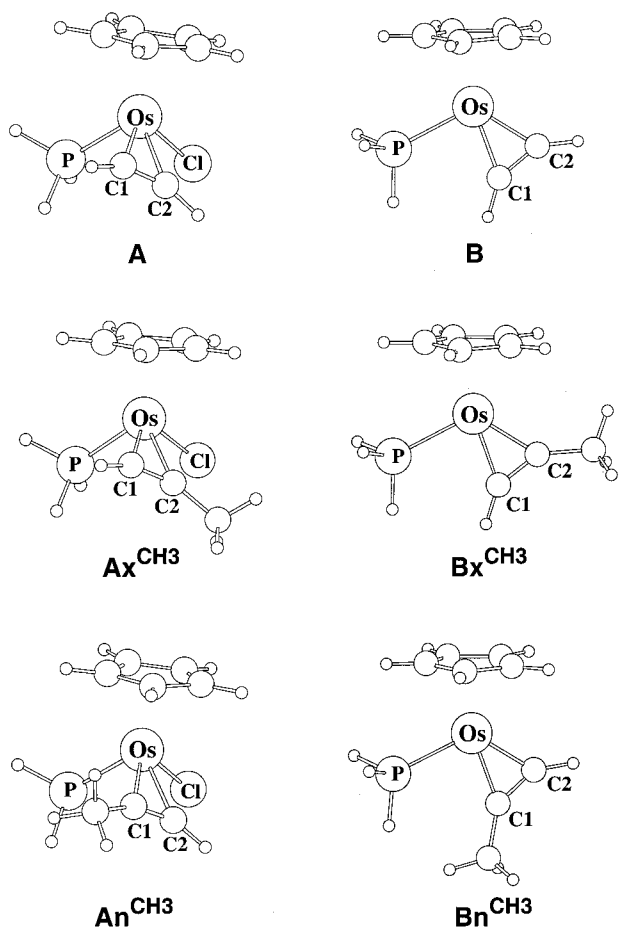


**Figure 3.** Optimized B3LYP geometries of the alkyne complexes  $\text{Os}(\eta^5\text{-C}_5\text{H}_5)\text{Cl}(\eta^2\text{-HC}\equiv\text{CR})(\text{PH}_3)$  ( $\text{R} = \text{H}$  (**A**),  $\text{CH}_3$  (**A**<sup>CH<sub>3</sub></sup>)) and  $[\text{Os}(\eta^5\text{-C}_5\text{H}_5)(\eta^2\text{-HC}\equiv\text{CR})(\text{PH}_3)]^+$  ( $\text{R} = \text{H}$  (**B**),  $\text{CH}_3$  (**B**<sup>CH<sub>3</sub></sup>)).

**Table 2.** Experimental and Calculated Geometric Parameters<sup>a</sup> and Calculated Bond Dissociation Energies<sup>b</sup>

param	1a	A	A <sub>x</sub> <sup>CH<sub>3</sub></sup>	2a	B	B <sub>x</sub> <sup>CH<sub>3</sub></sup>
Os–C1	2.142(7)	2.176	2.168	1.992	2.014	2.000
Os–C2	2.163(6)	2.150	2.182	1.981(8)	1.991	2.004
C1–C2	1.222(8)	1.265	1.266	1.26(2)	1.299	1.305
C1–C2–R	148.8(7)	152.6	152.4	140.3(9)	146.2	145.9
C2–C1–H	154(5)	152.6	152.0	145(4)	146.0	145.5
P–Os–C1–C2	112	106.0	105.7	183.7	179.9	180.1
<i>D<sub>e</sub></i>		23.0	21.1		69.6	71.1

<sup>a</sup> Bond lengths in Å and bond angles in degrees. <sup>b</sup> Alkyne–osmium bond dissociation energies (*D<sub>e</sub>*) in kcal mol<sup>−1</sup>.

result agrees with the experimental data, since the X-ray structures of complexes **1a** and **2a** correspond to exo forms. In the following, the discussion on substituted acetylenes will therefore concentrate on the exo isomers.

In Table 2 are summarized the most relevant theoretical parameters, together with those reported for experimental complexes **1a** and **2a**. Optimized geometries were found to be close to experimental ones for both alkyne complexes. The most interesting aspect of our computed geometrical parameters is that we succeeded in reproducing structural changes between complexes **1a** and **2a**. As we go from **A** to **B** the Os–C1 and Os–C2 distances decrease by 0.162 and 0.159 Å, respectively, and C1–C2 increases by only 0.034 Å. These results reflect the two-electron vs four-electron behavior of the alkyne ligand in complexes **A** and **B**, respectively.

It compares nicely with the geometry changes previously reported between  $\text{Os}(\text{CO})_4(\text{C}_2\text{H}_2)$  and  $\text{Os}(\text{CO})_3(\text{C}_2\text{H}_2)$  complexes<sup>19j</sup> at similar levels of calculation. In the former (two-electron-donor acetylene ligand), the Os–C (acetylene) bond distance is longer than in the latter (four-electron-donor acetylene ligand) by 0.189 Å (2.220 vs 2.031 Å), while the C–C distance is shorter by 0.053 Å (1.276 vs 1.329 Å). The bond length values for tetra- and tricarbonyl species are actually close to our computed values for complexes **A** and **B**, respectively (Table 2).

The coordination of the alkyne ligand induces not only a lengthening of the C1–C2 distance (1.18 Å in free alkyne)<sup>31</sup> but also a bending of the substituents away from the metal. The calculated bond angles of C2–C1–H moieties are 153° for complex **A** and 146° for **B**, in excellent agreement with the experimental values for **1a** (154(5)°) and **2a** (145(4)°). Finally, note that no significant differences in geometrical parameters were observed upon introduction of a methyl substituent onto the acetylene ligand (**A<sub>x</sub><sup>CH<sub>3</sub></sup>** and **B<sub>x</sub><sup>CH<sub>3</sub></sup>**).

It may be stated from the geometrical analysis that the behavior of the alkyne ligand as a donor of two or four electrons (2e or 4e) is reflected in both metal–carbon and carbon–carbon bond distances. Thus, when the alkyne acts as a 4e-donor ligand there is a contraction of the M–C bond, and the C–C bond is slightly elongated. The average experimental values of C–C distances in the coordinate terminal alkynes are 1.271 and 1.309 Å for 2e- and 4e-donor ligands, respectively.<sup>36</sup> It is interesting to notice that the X-ray-determined C–C distances for our osmium systems are shorter than these average values. Furthermore, the C–C distance of complex **2a**, in which the alkyne acts as a 4e-donor ligand, is in the range of the average value for 2e-donor ligands. The reliability of the C–C alkyne distance as an indicator of 2e- or 4e-donor ligand was studied by computing the monodimensional potential energy surface (PES) for the C–C coordinate in **A** and **B** complexes. The PES was built by varying the C–C distances from their equilibrium values and optimizing the rest of the complex at each point. The C–C distances that can be reached within an energy excess of 3 kcal mol<sup>−1</sup> with respect to the minimum energy structure range from 1.209 to 1.333 Å for complex **A** and from 1.243 to 1.378 Å for complex **B**. This is what we might call the flexibility range of the C≡C bond. The calculated PES is flat (Figure 4), and therefore, a wide range of C–C distances can be reached with low energy cost. Thus, the equilibrium distance of **A** (1.265 Å) is within the range of flexibility of **B**, and at the same time, the equilibrium distance of **B** (1.299 Å) is within the range of flexibility of complex **A**. The calculations show clearly that the C≡C bond lengths are not a reliable indicator of the metal–alkyne coordination mode.

Table 2 gives also the theoretically predicted alkyne bond dissociation energies (*D<sub>e</sub>*) of **A**, **B**, **A<sub>x</sub><sup>CH<sub>3</sub></sup>**, and **B<sub>x</sub><sup>CH<sub>3</sub></sup>**. The bond energies are calculated as the energy difference between the complex, on one hand, and the ligand and the metal fragment at their respective optimized geometries, on the other hand. The predicted

(36) Orpen, A. G.; Brammer, L.; Allen, F. H.; Kennard, O.; Watson, D. G.; Taylor, R. *J. Chem. Soc., Perkin Trans.* **1989**, S1.

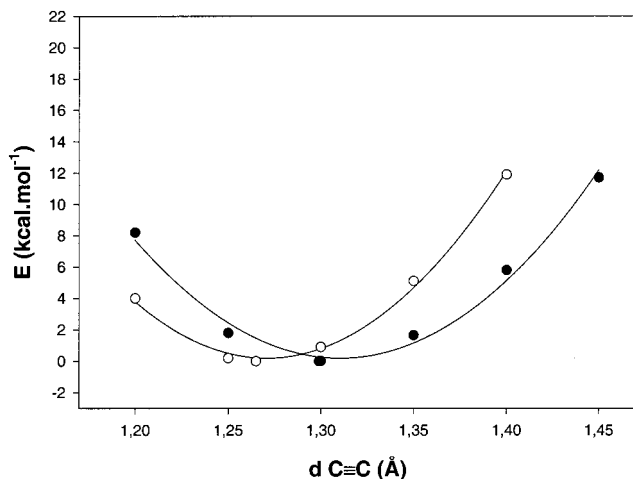


**Figure 4.** Potential energy surface for the C≡C distance in  $\text{Os}(\eta^5\text{-C}_5\text{H}_5)\text{Cl}(\eta^2\text{-HC}\equiv\text{CH})(\text{PH}_3)$  (○, **A**) and  $[\text{Os}(\eta^5\text{-C}_5\text{H}_5)(\eta^2\text{-HC}\equiv\text{CH})(\text{PH}_3)]^+$  (●, **B**) model systems.

$D_e$  for **B** (69.6 kcal mol<sup>-1</sup>) is substantially higher than  $D_e$  for the parent complex **A** (23.0 kcal mol<sup>-1</sup>). The stronger  $D_e$  of acetylene in **B** than in **A** can be attributed to the bond contribution of the acetylene second  $\pi$  system ( $\pi_{\perp}$ ) in the former. Similar bond energies were calculated for methyl-substituted acetylene: 21.1 and 71.1 kcal mol<sup>-1</sup> for **Ax**<sup>CH<sub>3</sub></sup> and **Bx**<sup>CH<sub>3</sub></sup>, respectively. It should be mentioned that the computed value of  $D_e$  for complex **B** (69.6 kcal mol<sup>-1</sup>) is higher than those usually reported in previous theoretical studies on alkyne–metal bonding.<sup>20</sup> However, in a recent contribution similar values were calculated at the CCSD(T) level for  $\text{Ni}(\text{C}_2\text{H}_2)_2$  and  $\text{Ni}(\text{PH}_3)_2(\text{C}_2\text{H}_2)_2$  complexes: 66.9 and 62.6 kcal mol<sup>-1</sup>, respectively.<sup>19i</sup> For both nickel complexes, this suggested a bonding contribution of acetylene's second  $\pi$  system. A bond-length/bond-strength correlation between the two acetylene complexes **A** and **B** is observed. The Os–C1 and Os–C2 bond distances of **B** are shorter than those of **A**, and the metal–acetylene  $D_e$  value of **B** is much higher than that of **A** (Table 2). Thus, a shortening of the osmium–alkyne distance increases the metal–ligand interaction. Therefore, we can state that the 4e alkyne ligands are more strongly bonded to the metal than their respective 2e alkyne ligands, due to the bonding contribution of the second  $\pi$  system of the alkyne.

**Rotational Barriers.** The transition states for the acetylene rotation were located for both **A** and **B** complexes and characterized by calculation of the Hessian matrix.

In complex **A**, the transition state (**Arot**, Figure 5) was found to be located 11.4 kcal mol<sup>-1</sup> above the minimum. In this structure, the dihedral angle between C≡C and Os–C1 bonds is equal to 50.7°. The values of the Os–C(acetylene) distances are 2.300 and 2.198 Å, and the C≡C distance is 1.245 Å. Comparison with the geometry of the minimum energy structure **A** (Table 2) shows that the rotation induces a lengthening of the M–C distances accompanied by a shortening of the C–C distance. These changes between **A** and **Arot** can be rationalized by the orbital arguments developed by Hoffmann et al.:<sup>34</sup> the lengthening of the Os–C distances upon rotation of the acetylene ligand results from the increase of the Os– $\pi_{\perp}$  repulsive interaction, while the shortening of the C≡C bond is related to the

decrease of the back-donation to the  $\pi_{\parallel}^*$  orbital. **Arot** remains, however, an 18-electron species in which the acetylene acts as a 2-electron-donor ligand.

The situation is more complicated for complex **B**, since *two* saddle points were characterized for the rotational process of acetylene. In the first one (**Brot**, Figure 5), the optimized geometrical parameters are rather similar to those given just above for **Arot**, with Os–C(acetylene) distances of 2.186 and 2.283 Å and a C–C distance of 1.249 Å. Despite this geometrical similarity, the computed energy barrier is much higher, since **Brot** is located 32.7 kcal mol<sup>-1</sup> above the minimum energy structure **B**. This remarkably high value for the rotational barrier can be explained by using the symmetry properties of the fragment molecular orbitals displayed in Figure 2. We have previously mentioned that in the equilibrium structure **B** the filled  $\pi$  orbitals,  $\pi_{\parallel}$  and  $\pi_{\perp}$ , are respectively symmetric (*a'*) and antisymmetric (*a''*) with respect to the molecular symmetry plane, so that each of them can interact with one of the two low-lying *d* orbitals of the metal fragment ( $\pi_{\perp}$  with *a''* and  $\pi_{\parallel}$  with *1a'*; Figure 2). Therefore, in the equilibrium structure, the acetylene ligand plays the role of a four-electron donor. In the transition state structure, the acetylene is rotated by 90°. Assuming an idealized  $C_s$  symmetry, both  $\pi_{\parallel}$  and  $\pi_{\perp}$  become symmetric, so that the overlap between  $\pi_{\perp}$  and the *a''* metal fragment orbital vanishes. The electron donation from  $\pi_{\perp}$  is thus lost, and the only significant interaction which remains is that between  $\pi_{\parallel}$  and the *1a'* orbital. The high value computed for the rotational barrier can thus be traced to the change of the electron donor character of the acetylene ligand on going from **B** (4-electron, 18-electron species) to **Brot** (2-electron, 16-electron species). This qualitative analysis, consistent with the evolution of the geometrical parameters, is further supported by the NBO analysis. The population of the alkyne  $\pi_{\perp}$  NBO is significantly smaller for complex **B** (1.679e) than for the transition state **Brot** (1.984e), in which this orbital is almost full. These results show that  $\pi_{\perp}$  is involved in alkyne–metal bonding in the stable complex, **B**, but not in the **Brot** structure.

As mentioned above, a second transition state was found for the acetylene rotation (**Brot'**, Figure 5). Its geometry strongly differs from that of **Brot**: the Os–C(acetylene) distances (1.930 and 1.929 Å) are shortened about 0.3 Å, and the C–C distance (1.362 Å) is lengthened by 0.113 Å. Note that this latter value is greater than that for free ethylene (1.336 Å). These geometrical features clearly indicate that the nature of the metal–acetylene bonding in **Brot'** cannot be described in terms of donor–acceptor interactions following the Dewar–Chatt–Duncanson model.<sup>37</sup> It is better to consider **Brot'** as a metallacycle with two Os–C single bonds and a double bond between the carbon atoms, instead of an alkyne complex. Last but not least, **Brot'** was found to be lower in energy than **Brot** by 8.4 kcal mol<sup>-1</sup>. Consequently, the lowest energy path for the rotation of the alkyne ligand in complex **B** involves the metallacycle **Brot'** as a transition state structure. The activa-

(37) (a) Dewar, M. J. S. *Bull. Soc. Chim. Fr.* **1951**, *18*, C79. (b) Chatt, J.; Duncanson, L. A. *J. Chem. Soc.* **1953**, 2939.



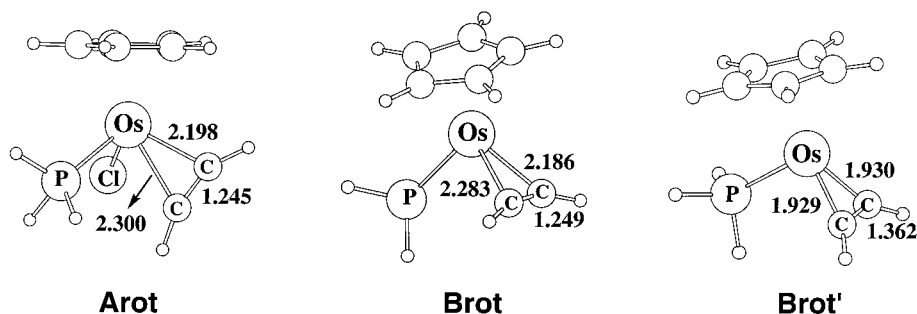


**Figure 5.** Optimized B3LYP geometries of **Arot**, **Brot**, and **Brot'** structures. Bond distances are given in Å.

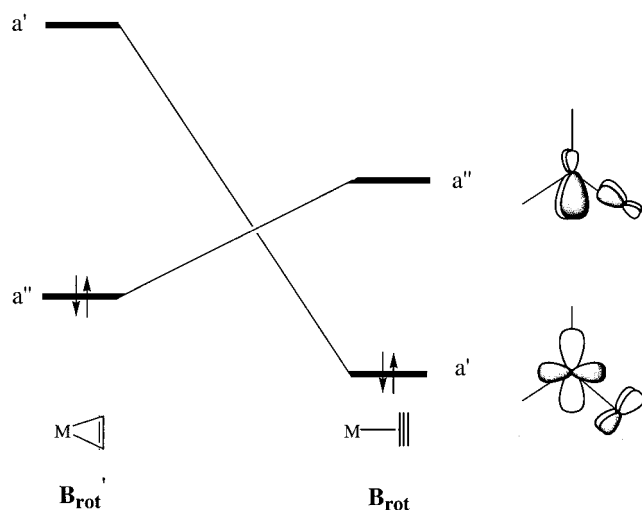


**Figure 6.** Schematic drawing of the frontier molecular orbital crossing found on going from **Brot** to **Brot'**.

tion energy remains high (24.3 kcal mol<sup>-1</sup>) compared to that for complex **A**, because **Brot'** is still a 16-electron species.

**Brot** and **Brot'** can be seen as two structures along the reaction path for the perpendicular approach of an acetylene molecule toward the CpOs(PH<sub>3</sub>)<sup>+</sup> metal fragment. Since both have been characterized as saddle points for the acetylene rotational process, this means that an energy barrier should be encountered on going from **Brot** to **Brot'** by decreasing the Os–acetylene distance. The origin of this barrier, which makes it possible to optimize separately an acetylene (**Brot**) and a metallacyclopropene (**Brot'**) complex, lies in a *change of the ground electronic configuration*, schematically depicted in Figure 6, which in turn reflects the different chemical natures of the two complexes. Let us assume an idealized C<sub>s</sub> symmetry to analyze the origin of this orbital crossing. In **Brot** (“long” Os–C distance), the HOMO (a') is the antibonding combination of the filled π<sub>⊥</sub> ligand orbital with a filled metal fragment orbital and the LUMO (a'') a bonding combination of π<sub>||</sub>\* with the filled a'' orbital on the metal fragment (Figure 6, right-hand side). Going from **Brot** to **Brot'** entails a shortening of Os–C distances and a lengthening of the C–C distance. The HOMO (a'), Os–C antibonding and C–C bonding, is thus destabilized, while the LUMO (a''), Os–C bonding and C–C antibonding, is stabilized. A crossing occurs between these occupied and vacant molecular orbitals, which results in an energy barrier between these two structures (reaction path “forbidden by symmetry”). Note that in turn the change from a'<sup>2</sup> to a''<sup>2</sup> ground-state configuration is consistent with a

**Table 3.** NMR <sup>13</sup>C and <sup>1</sup>H Chemical Shifts (ppm) Relative to TMS, and NPA Charges<sup>a</sup>

param	1a	1b	A	Ax <sup>CH3</sup>	2a	2b	B	Bx <sup>CH3</sup>
δ( <sup>13</sup> C) C1	57.5	49.6	68.7	57.7	146.0	143.3	145.3	144.8
δ( <sup>13</sup> C) C2	82.2	69.1	104.2	102.6	179.0	182.8	157.3	175.0
δ( <sup>1</sup> H) H <sup>b</sup>	4.32	3.72	4.4	3.7	9.43	9.9	8.9	8.8
q(C1) <sup>c</sup>			-0.08	-0.10			-0.04	-0.05
q(C2) <sup>c</sup>			0.04	0.00			0.05	0.10
q(H)			0.25	0.25			0.28	0.28

<sup>a</sup> Charges in atomic units. <sup>b</sup> Chemical shifts for terminal acetylenic hydrogens. <sup>c</sup> The charges of the substituents have been added to the charges of acetylenic carbons.

shortening of the M–C(acetylene) distances (antibonding M–C → bonding M–C) and a lengthening of the C–C distance (bonding C–C → antibonding C–C) on going from **Brot** to **Brot'**.

**NMR Properties.** We have carried out theoretical studies on the NMR properties of model complexes **A**, **Ax<sup>CH3</sup>**, **B**, and **Bx<sup>CH3</sup>** by using the gauge-including atomic orbitals (GIAO) method.<sup>38</sup> The <sup>13</sup>C and <sup>1</sup>H chemical shifts were calculated with respect to tetramethylsilane. Recently, the GIAO method has been successfully used in the study of NMR properties of acetylenes coordinated to a transition metal by Walther and co-workers.<sup>19i</sup>

Table 3 collects the experimental and calculated chemical shifts, as well as the NPA charges on acetylenic carbons. The calculated chemical shifts are in the range found experimentally and reproduce the trend observed on going from **1** to **2**. Calculated δ(<sup>13</sup>C) values for **B** (145.3 and 157.3 ppm) are significantly higher than those for **A** (68.7 and 104.2 ppm). The same trend is observed for the calculated δ(<sup>1</sup>H) values: 4.4 ppm for **A** and 8.9 ppm for **B**. When a methyl group replaces one of the acetylenic hydrogens (**Ax<sup>CH3</sup>** and **Bx<sup>CH3</sup>**), δ-(<sup>13</sup>C) and δ(<sup>1</sup>H) still better fit the experimental values. The NMR properties are very sensitive to electronic variations, and therefore, the use of a simple alkyne model could be one source of error on computed chemical shifts, especially for substituted acetylenic carbons. However, we have succeeded in reproducing qualitatively the differences between a two-electron-donor and a four-electron-donor alkyne complex.

Additionally, we have computed the <sup>13</sup>C and <sup>1</sup>H chemical shifts of the saddle points for acetylene rotation (**Arot**, **Brot** and **Brot'**). The average values of the calculated δ(<sup>13</sup>C) for acetylenic carbons of **Arot** species (77.8 ppm) and **Brot** species (69.7 ppm) are similar and are more closely related to complex **A** than to complex **B** (Table 3). On the other hand, the average value for

(38) Shreckenbach, G.; Ziegler, T. *J. Phys. Chem.* **1995**, *99*, 606.

**Brot'** (249.3 ppm) is much higher than those computed for **A** and **B** complexes. These results indicate that the bonding scheme in **Arot** and **Brot** structures resembles that in complex **A**, in which the acetylene ligand acts as a two-electron donor, while the scheme in **Brot'** differs from those in **A** and **B**. Thus, computed NMR properties further support the arguments stated in the previous section about the bonding nature of rotational structures.

The  $^{13}\text{C}$  chemical shift values are roughly indicative of the electronic density around that atom. The atom most shifted is the least shielded one and, consequently, the poorest in electrons. Thus, one could expect a correlation between the atomic charges and the chemical shift of the acetylenic coordinated carbons, in such a way that the least charged carbon is the most shifted. The calculated NPA charges of acetylenic carbons are consistent with this argument for a given complex (Table 3). Also, NPA charges show that acetylenic carbons are less charged for the 4e donor acetylene complex **B** ( $-0.04\text{e}$  and  $0.05\text{e}$ ) than for the 2e donor **A** ( $-0.08\text{e}$  and  $0.04\text{e}$ ), the **B** complex exhibiting the most shifted carbons. Despite variations in atomic carbon charges, the small differences ( $\leq 0.04\text{e}$ ) do not seem to justify the considerable variation in chemical shifts observed for the two bonding situations. Note, however, that the two complexes carry different total net charges, which could mask the differences in atomic charges, hindering a direct comparison between them. Apart from atomic charges, chemical shifts may be also related to the occupancies of acetylenic molecular orbitals. From the NBO analysis we found that in complex **B** the  $\pi_{\perp}$  orbital is significantly depopulated ( $1.679\text{e}$ ), while that for complex **A** is full ( $1.982\text{e}$ ). Thus, in line with previous arguments, when the alkyne ligand acts as a four-electron donor there is a decrease of electron population on acetylenic carbons, which become more deshielded and, consequently, appear at low-field resonance: i.e., highly shifted.

**Bader Analysis.** The metal–alkyne bonding has been also investigated by means of Bader analysis of the electron density. Bader's atoms in molecules (AIM) theory provides a set of practical tools for the study of bonding properties.<sup>39</sup> The Os–C and C≡C interactions were characterized by critical points (cp's) in the electronic charge density ( $\rho(r)$ ), which are points in the space where  $\nabla\rho(r)$  vanishes. According to Bader's theory, the localization of a bond critical point (bcp) between two atoms proves the existence of an interaction between them, while the ring critical point (rcp) is characteristic of atomic rings. The values of  $\rho(r)$ , Laplacian ( $\nabla^2\rho(r)$ ), and ellipticity ( $\epsilon$ ) at the critical points were used to gauge the variation in charge density and bonding properties for the complexes under study. In Table 4 are summarized the results of topological analysis of electron density, for acetylene and propyne complexes, as well as for the saddle points of the rotational process. In a first inspection of the data collected in Table 4, some general trends can be observed. The values of the Laplacian at the bcp ( $\nabla^2\rho_{\text{CP}}$ ) are relatively low and positive for all the Os–C(alkyne) bonds, except for the

**Table 4. Topological Properties of the Electron Density at the Bond and Ring Critical Points<sup>a</sup>**

		<b>A</b>	<b>Ax<sup>CH3</sup></b>	<b>Arot</b>	<b>B</b>	<b>Bx<sup>CH3</sup></b>	<b>Brot</b>	<b>Brot'</b>
Os–C1	$\rho_{\text{CP}}$	0.097	0.099	0.075	0.138	0.142	0.075	0.165
	$\nabla^2\rho_{\text{CP}}$	0.158	0.143	0.161	0.185	0.177	0.170	0.272
Os–C2	$\rho_{\text{CP}}$	0.101	0.096	0.090	0.143	0.140	0.091	0.164
	$\nabla^2\rho_{\text{CP}}$	0.180	0.174	0.153	0.212	0.205	0.155	0.276
C1–Os–C2 <sup>b</sup>	$\rho_{\text{CP}}$	0.090	0.089	0.074	0.124	0.124	0.075	0.144
	$\nabla^2\rho_{\text{CP}}$	0.360	0.348	0.276	0.472	0.469	0.248	0.505
C1–C2	$\rho_{\text{CP}}$	0.377	0.376	0.388	0.363	0.359	0.373	0.328
	$\nabla^2\rho_{\text{CP}}$	-1.041	-1.095	-1.156	-1.041	-1.021	-1.096	-0.856
	$\epsilon$	0.189	0.210	0.183	0.024	0.030	0.145	0.075

<sup>a</sup> Electron charge density  $\rho_{\text{CP}}$ , Laplacian  $\nabla^2\rho_{\text{CP}}$ , and ellipticity  $\epsilon$ , in atomic units. <sup>b</sup> Ring critical point.

**Brot'** structure. Thus, according to AIM theory, the relatively low and positive value of the Laplacian at the bcp indicates a closed-shell interaction. On the other hand, for C≡C bonds the values of  $\nabla^2\rho_{\text{CP}}$  (large and negative) are indicative of shared interactions, characterized by a large accumulation of charge between the nuclei.

The two kinds of acetylene complexes, **A** and **B**, present differences in the topological properties of electron density for the osmium–acetylene interactions. Larger values of  $\rho(r)$  at the bcp ( $\rho_{\text{CP}}$ ) for Os–C bonds are observed in the four-electron-donor acetylene complex **B** (Table 4). The value of  $\rho_{\text{CP}}$  is related to the bond order and can be considered a measure of the bond strength, in such a way that the larger  $\rho_{\text{CP}}$  is, the stronger the bond. Thus, these results are consistent with our previous findings, which indicated an increase in the strength of the metal–acetylene bond when the  $\pi_{\perp}$  orbital participated in the bonding. The calculated values of  $\rho_{\text{CP}}$  for Os–C bonds increase by  $0.04\text{e}$ , from  $0.097\text{e}$  and  $0.101\text{e}$  in **A** to  $0.138\text{e}$  and  $0.143\text{e}$  in **B**. These values compare nicely with those reported by Decker and Klobukowski for  $\text{Ru}(\text{CO})_4(\text{C}_2\text{H}_2)$  and  $\text{Ru}(\text{CO})_3(\text{C}_2\text{H}_2)$  complexes,<sup>19j</sup> in which it was found that the acetylene ligand acts as a two-electron and four-electron donor, respectively. In the Ru complexes the  $\rho_{\text{CP}}$  values increase also by  $0.04\text{e}$ , from  $0.075\text{e}$  in the tetracarbonyl complex to  $0.110\text{e}$  in the tricarbonyl species. Moreover, ring critical points were found between the Os and the acetylenic carbons, and a larger value of  $\rho_{\text{CP}}$  was observed in complex **B** for the metallacyclopropene-like ring. For C–C acetylene bonds the value of  $\rho_{\text{CP}}$  decreases on going from complex **A** to **B**, suggesting a weakening of the acetylene bond. However, the decrease in the amount of  $\rho_{\text{CP}}$  is small, only  $0.01\text{e}$  (from  $0.377\text{e}$  in **A** to  $0.363\text{e}$  in **B**). This is not surprising, since we have shown in a previous section that the C≡C bond is relatively flexible: i.e., that a wide range of C–C distances can be reached with low energy cost. Neither the C–C bond lengths nor the values of  $\rho(r)$  at the C–C bcp are reliable indicators of the metal–alkyne coordination mode. In spite of this, significant differences were found in the values of ellipticity ( $\epsilon$ ) for the C–C bonds between the two complexes (Table 4). The ellipticity provides a measure for the  $\pi$  character of the bond; thus, large values of ellipticity are indicative of high  $\pi$  bond character. The low value of  $\epsilon$  at the C–C bcp in **B** ( $0.024\text{e}$ ) can be related to the participation of two  $\pi$  orbitals instead of one in the bonding, which will decrease the  $\pi$  character of the acetylene. We have focused our discussion on the topological analysis of

(39) (a) Bader, R. F. W. *Atoms in Molecules: A Quantum Theory*; Clarendon Press: Oxford, U.K., 1990. (b) Bader, R. F. W. *Chem. Rev.* **1992**, *92*, 893.



acetylenic complexes; however, the same argument could be drawn for the methyl-substituted acetylenic complexes **Ax**<sup>CH<sub>3</sub></sup> and **Bx**<sup>CH<sub>3</sub></sup>. In summary, the differences in coordination mode of the alkyne complexes are reflected in the properties of the electron density topology, in both the values of  $\rho_{CP}$  at the Os–C bonds and of  $\epsilon$  at the C–C bcp. Therefore, when the two  $\pi$  orbitals of alkyne participate in the bonding, higher values of  $\rho_{CP}$  and lower values of  $\epsilon$  are expected.

Additionally, we have performed the topological analysis of electron density for osmium–acetylene interactions in the saddle points for acetylene rotation (**Arot**, **Brot**, and **Brot'**). The topological properties in **Arot** and **Brot** species are very similar for both  $\rho(r)$  and  $\epsilon$  at the bcp's. The values of  $\rho_{CP}$  at the Os–C bonds and  $\epsilon$  at the C–C bcp's better compare to the values found in the acetylene complex **A** than in **B**, further proving the two-electron coordination of acetylene in these rotational species. However, somewhat lower values of  $\rho_{CP}$  at the Os–C bonds were observed in **Arot** and **Brot**, indicating a weakening of the Os–acetylene bonding. The **Brot'** structure presents a significant increase in the values of  $\rho_{CP}$  at the Os–C bonds and a decrease at the C–C acetylenic bonds, reaching respectively higher and lower values than those of complex **B**. In addition relatively large values of  $(\nabla^2\rho_{CP})$  at the Os–C bonds were observed, suggesting a change in the nature of the metal–alkyne interaction for **Brot'** species, in agreement with previous findings.

### Concluding Remarks

Treatment of the  $\pi$ -alkyne complexes  $\text{Os}(\eta^5\text{-C}_5\text{H}_5)\text{Cl}\{\eta^2\text{-HC}\equiv\text{CC}(\text{OH})\text{R}_2\}(\text{P}^i\text{Pr}_3)$  (**1**) with  $\text{TiPF}_6$  produces the extraction of the chloride ligand and the formation of  $[\text{Os}(\eta^5\text{-C}_5\text{H}_5)\{\eta^2\text{-HC}\equiv\text{CC}(\text{OH})\text{R}_2\}(\text{P}^i\text{Pr}_3)]\text{PF}_6$  (**2**). The extraction of the chloride ligand from **1** generates an interaction between an empty d orbital of the osmium atom and the  $\pi_{\perp}$  orbital of the alkyne. As a result, the structural parameters and the spectroscopic properties of the alkyne undergo significant disturbances. The Os–alkyne distances are shortened, and in the  $^{13}\text{C}\{^1\text{H}\}$  and  $^1\text{H}$  NMR spectra, the chemical shifts of the acetylenic carbon and  $\text{HC}\equiv$  resonances are shifted toward lower field. Theoretical calculations on the model compounds  $\text{Os}(\eta^5\text{-C}_5\text{H}_5)\text{Cl}\{\eta^2\text{-HC}\equiv\text{CR}\}(\text{PH}_3)$  (**A**) and  $[\text{Os}(\eta^5\text{-C}_5\text{H}_5)\{\eta^2\text{-HC}\equiv\text{CR}\}(\text{PH}_3)]^+$  (**B**) suggest that the disturbance in the chemical shifts is a consequence of the depopulation of the  $\pi_{\perp}$  orbital of the alkyne, on going from **1** to **2** or from **A** to **B**. Both structural and spectroscopic changes are in accord with the rationale of an increased donation from the alkyne, as a consequence of the participation of the acetylenic second  $\pi$  orbital ( $\pi_{\perp}$ ) in the bonding.

The theoretical calculations also predict that, in these types of systems, the interaction between the  $\pi_{\perp}$  orbital of the alkyne and an empty d orbital of the osmium gives rise to an increase of the dissociation energy of the alkyne and an increase of the energy for the rotation of the alkyne around the osmium–alkyne axis. The enhancement in the rotational barrier is due to the loss of the  $\pi_{\perp}\rightarrow\text{M}$  interaction, which makes rotation proceed via a formally unsaturated 16-electron path. The results of topological properties of the electron density of the system also reflect the  $\pi_{\perp}\rightarrow\text{M}$  interaction and are in full

agreement with previous findings. As we go from **A** to **B**, we observe an increase of electron density at the bcp between the metal and the acetylenic carbon atoms, which is accompanied by a decrease of  $\epsilon$  at the bcp between the two acetylenic carbons. These results are consistent with an increase in the amount of bonding between the alkyne ligand and the metal.

### Experimental Section

**Synthesis.** All reactions were carried out with exclusion of air using standard Schlenk techniques. Solvents were dried by known procedures and distilled under argon prior to use. The complexes  $\text{Os}(\eta^5\text{-C}_5\text{H}_5)\text{Cl}\{\eta^2\text{-HC}\equiv\text{CC}(\text{OH})\text{Ph}_2\}(\text{P}^i\text{Pr}_3)^{27b}$  (**1a**) and  $\text{Os}(\eta^5\text{-C}_5\text{H}_5)\text{Cl}\{\eta^2\text{-HC}\equiv\text{CC}(\text{OH})(\text{CH}_3)_2\}(\text{P}^i\text{Pr}_3)^{28}$  (**1b**) were prepared as previously reported.

In the NMR spectra, chemical shifts are expressed in ppm downfield from tetramethylsilane ( $^1\text{H}$  and  $^{13}\text{C}\{^1\text{H}\}$ ) and  $\text{H}_3\text{-PO}_4$  (85%) ( $^{31}\text{P}\{^1\text{H}\}$ ).

**Preparation of  $[\text{Os}(\eta^5\text{-C}_5\text{H}_5)\{\eta^2\text{-HC}\equiv\text{CC}(\text{OH})\text{Ph}_2\}(\text{P}^i\text{Pr}_3)]\text{PF}_6$  (**2a**).** A solution of  $\text{Os}(\eta^5\text{-C}_5\text{H}_5)\text{Cl}\{\eta^2\text{-HC}\equiv\text{CC}(\text{OH})\text{Ph}_2\}(\text{P}^i\text{Pr}_3)$  (**1a**; 125 mg, 0.19 mmol) in 10 mL of dichloromethane was treated with  $\text{TiPF}_6$  (67 mg, 0.19 mmol). The mixture was stirred for 2 min and then filtered through Kieselguhr and concentrated to dryness. The residue was washed with diethyl ether to yield a pale brown solid. Yield: 118 mg (81%). IR (Nujol):  $\nu(\text{OH})$  3529,  $\nu(\text{PF}_6)$  840  $\text{cm}^{-1}$ .  $^1\text{H}$  NMR (300 MHz,  $\text{CD}_2\text{Cl}_2$ , 293 K):  $\delta$  9.43 (d, 1 H,  $J(\text{PH}) = 26.4$  Hz,  $\equiv\text{CH}$ ), 7.30 (br s, 10 H, Ph), 5.39 (s, 5 H, Cp), 3.62 (s, 1 H, OH), 2.65 (m, 3 H, PCH), 1.16 (dd, 18 H,  $J(\text{HH}) = 7.2$  Hz,  $J(\text{PH}) = 14.7$  Hz, PCCH<sub>3</sub>).  $^{31}\text{P}\{^1\text{H}\}$  NMR (121.4 MHz,  $\text{CD}_2\text{Cl}_2$ , 293 K):  $\delta$  38.0 (s),  $-144.7$  (sept,  $J(\text{PF}) = 713$  Hz,  $\text{PF}_6$ ).  $^{13}\text{C}\{^1\text{H}\}$  NMR (75.4 MHz,  $(\text{CD}_3)_2\text{CO}$ , 223 K):  $\delta$  179.0 (s,  $\equiv\text{C}-$ ), 147.7 (s, ipso-Ph), 146.0 (s,  $\equiv\text{CH}$ ), 129.0, 128.3, 126.8 (all s, Ph), 84.9 (s, COH), 77.1 (s, Cp), 26.2 (br, PCH), 19.7 (br, PCCH<sub>3</sub>). Anal. Calcd for  $\text{C}_{29}\text{H}_{38}\text{F}_6\text{OOSp}_2$ : C, 45.31; H, 4.98. Found: C, 45.08; H, 5.09. MS (FAB<sup>+</sup>):  $m/e$  625 ( $\text{M}^+$ ).

**Preparation of  $[\text{Os}(\eta^5\text{-C}_5\text{H}_5)\{\eta^2\text{-HC}\equiv\text{CC}(\text{OH})(\text{CH}_3)_2\}(\text{P}^i\text{Pr}_3)]\text{PF}_6$  (**2b**).** A solution of  $\text{Os}(\eta^5\text{-C}_5\text{H}_5)\text{Cl}\{\eta^2\text{-HC}\equiv\text{CC}(\text{OH})(\text{CH}_3)_2\}(\text{P}^i\text{Pr}_3)$  (**1b**; 128 mg, 0.24 mmol) in 10 mL of dichloromethane was treated with  $\text{TiPF}_6$  (84 mg, 0.24 mmol). The mixture was stirred for 2 min and then filtered through Kieselguhr and concentrated to dryness. The residue was washed with diethyl ether to yield a pale brown solid. Yield: 135 mg (87%). IR (Nujol):  $\nu(\text{OH})$  3575,  $\nu(\text{PF}_6)$  840  $\text{cm}^{-1}$ .  $^1\text{H}$  NMR (300 MHz,  $\text{CD}_2\text{Cl}_2$ , 293 K):  $\delta$  9.17 (br d, 1 H,  $J(\text{PH}) = 26.4$  Hz,  $\equiv\text{CH}$ ), 5.70 (s, 5 H, Cp), 5.67 (s, 1 H, OH), 2.70 (m, 3 H, PCH), 1.70 (s, 6 H, CH<sub>3</sub>), 1.23 (dd, 18 H,  $J(\text{HH}) = 7.2$  Hz,  $J(\text{PH}) = 14.4$  Hz, PCCH<sub>3</sub>).  $^{31}\text{P}\{^1\text{H}\}$  NMR (121.4 MHz,  $\text{CD}_2\text{Cl}_2$ , 293 K):  $\delta$  36.3 (s),  $-144.7$  (sept,  $J(\text{PF}) = 713$  Hz,  $\text{PF}_6$ ).  $^{13}\text{C}\{^1\text{H}\}$  NMR (75.4 MHz,  $\text{CD}_2\text{Cl}_2$ , 223 K):  $\delta$  182.8 (s,  $\equiv\text{C}-$ ), 143.3 (s,  $\equiv\text{CH}$ ), 77.6 (s, COH), 76.4 (s, Cp), 31.6 (s, CH<sub>3</sub>), 27.3 (br d,  $J(\text{PC}) = 29.7$  Hz, PCH), 20.0 (s, PCCH<sub>3</sub>). Anal. Calcd for  $\text{C}_{19}\text{H}_{34}\text{F}_6\text{OOSp}_2$ : C, 35.40; H, 5.32. Found: C, 35.35; H, 5.41. MS (FAB<sup>+</sup>):  $m/e$  501 ( $\text{M}^+$ ).

**Crystal Data.** Crystals suitable for X-ray diffraction were obtained by slow diffusion of pentane into a concentrated solution of **1a** in toluene or by diffusion of diethyl ether into a concentrated solution of **2a** in  $\text{CH}_2\text{Cl}_2$ . A summary of crystal data and refinement parameters is listed in Table 5. Data were collected on a Siemens Stoe AED-2 diffractometer, with graphite-monochromated Mo K $\alpha$  radiation ( $\lambda = 0.71073$  Å), using the  $\omega/2\theta$  scan method. Three standard reflections were monitored every 55 min throughout data collection; no important variations were observed. Both data were corrected for Lorentz and polarization effects and for absorption using the  $\psi$ -scan method. Both structures were solved by Patterson and Fourier techniques and refined by full-matrix least-squares

**Table 5. Crystallographic Data for  $\text{Os}(\eta^5\text{-C}_5\text{H}_5)\text{Cl}\{\eta^2\text{-HC}\equiv\text{CC}(\text{OH})\text{Ph}_2\}(\text{P}^i\text{Pr}_3)$  (**1a**) and  $[\text{Os}(\eta^5\text{-C}_5\text{H}_5)\{\eta^2\text{-HC}\equiv\text{CC}(\text{OH})\text{Ph}_2\}(\text{P}^i\text{Pr}_3)]\text{PF}_6$  (**2a**)**

	<b>1a</b>	<b>2a</b>
formula	C <sub>29</sub> H <sub>38</sub> ClO <sub>3</sub> OsP	C <sub>29</sub> H <sub>38</sub> F <sub>6</sub> O <sub>3</sub> OsP <sub>2</sub>
<i>M<sub>r</sub></i>	659.21	768.63
<i>T</i> (K)	295	295
cryst syst	orthorhombic	orthorhombic
space group	<i>Pbca</i>	<i>Pna2<sub>1</sub></i>
<i>a</i> , Å	13.924(2)	16.842(2)
<i>b</i> , Å	17.670(2)	9.077(2)
<i>c</i> , Å	22.157(3)	19.643(3)
<i>V</i> , Å <sup>3</sup>	5451.4(12)	3002.9(6)
<i>Z</i>	8	4
$\rho_{\text{calcd}}$ (g cm <sup>-3</sup> )	1.606	1.700
$\mu$ , mm <sup>-1</sup>	4.85	4.41
$\theta$ , range data collectn (deg)	2–25	2–25
no. of measd rflns	10 237	8554
no. of unique rflns	4798	5282
no. of restraints/params	282/2	333/5
<i>R</i> ( <i>F</i> ) ( $F^2 > 2\sigma(F^2)$ ) <sup>a</sup>	0.0351	0.0788
<i>R<sub>w</sub></i> ( $F^2$ ) (all data) <sup>b</sup>	0.0351	0.0340

<sup>a</sup>  $R(F) = \sum ||F_o| - |F_c|| / \sum |F_o|$ . <sup>b</sup>  $R_w(F^2) = (\sum [w(F_o^2 - F_c^2)^2] / \sum [w(F_o^2)^2])^{1/2}$ .

on  $F^2$ .<sup>40</sup> Atomic scattering factors, corrected for anomalous dispersion, were used as implemented in the refinement program.

Crystals of approximate dimensions 0.37 × 0.19 × 0.11 mm (**1a**) and 0.22 × 0.20 × 0.19 mm (**2a**) were used for data collection. Cell constants were obtained by the least-squares fit on the setting angles of 60 reflections in the range 20 ≤ 2θ ≤ 40° (**1a** and **2a**). Data were collected at room temperature in the range 4 ≤ 2θ ≤ 50° (−16 ≤ *h* ≤ 16, 0 ≤ *k* ≤ 21, 0 ≤ *l* ≤ 26; 10 237 measured reflections, 4798 unique ( $R_{\text{int}} = 0.0377$ )) for **1a**; or in the range 4 ≤ 2θ ≤ 50° (0 ≤ *h* ≤ 20, −10 ≤ *k* ≤ 4, −23 ≤ *l* ≤ 23; 8554 measured reflections, 5282 unique ( $R_{\text{int}} = 0.0377$ )) for **2a**. In both molecules a phenyl group of the alkynol ligand was observed to be disordered, and both were refined with two moieties (A and B), with complementary occupancy factors and restrained geometry. In **2a**, the PF<sub>6</sub> anion was observed to be disordered in the same way, also. Anisotropic displacement parameters were used in the last cycles of refinement for all hydrogen atoms, except those involved in disorder. Hydrogen atoms, except the alkynol ones, were placed in calculated positions and refined riding on the corresponding carbon atoms.

**Computational Details.** Calculations were performed with the GAUSSIAN 98 series of programs<sup>41</sup> within the framework of density functional theory (DFT)<sup>42</sup> using the B3LYP functional.<sup>43</sup> A quasi-relativistic effective core potential operator

(40) Sheldrick, G. M. University of Göttingen, Göttingen, Germany, 1997.

(41) Frisch, M. J.; Trucks, G. W.; Schlegel, H. B.; Scuseria, G. E.; Robb, M. A.; Cheeseman, J. R.; Zakrzewski, V. G.; Montgomery, J. A., Jr.; Stratmann, R. E.; Burant, J. C.; Dapprich, S.; Millam, J. M.; Daniels, A. D.; Kudin, K. N.; Strain, M. C.; Farkas, O.; Tomasi, J.; Barone, V.; Cossi, M.; Cammi, R.; Mennucci, B.; Pomelli, C.; Adamo, C.; Clifford, S.; Ochterski, J.; Petersson, G. A.; Ayala, P. Y.; Cui, Q.; Morokuma, K.; Malick, D. K.; Rabuck, A. D.; Raghavachari, K.; Foresman, J. B.; Cioslowski, J.; Ortiz, J. V.; Stefanov, B. B.; Liu, G.; Liashenko, A.; Piskorz, P.; Komaromi, I.; Gomperts, R.; Martin, R. L.; Fox, D. J.; Keith, T.; Al-Laham, M. A.; Peng, C. Y.; Nanayakkara, A.; Gonzalez, C.; Challacombe, M.; Gill, P. M. W.; Johnson, B. G.; Chen, W.; Wong, M. W.; Andres, J. L.; Head-Gordon, M.; Replogle, E. S.; Pople, J. A. *Gaussian 98*; Gaussian, Inc.: Pittsburgh, PA, 1998.

was used to represent the 60 innermost electrons of the osmium atom.<sup>44</sup> The basis set for the metal atom was that associated with the pseudopotential,<sup>44</sup> with a standard double- $\zeta$  LANL2DZ contraction.<sup>41</sup> The 6-31G(d,p) basis set was used for the P, Cl, and C atoms directly attached to the metal, whereas the 6-31G basis set was used for the hydrogen atoms.<sup>45</sup> In the case of propyne model complexes (**A**<sup>CH<sub>3</sub></sup> and **B**<sup>CH<sub>3</sub></sup>) the C and H atoms of the methyl substituents were described using a 6-31G basis set.<sup>45</sup> Geometry optimizations were carried out without any symmetry restrictions, and all stationary points were optimized with analytical first derivatives. Saddle points were located by means of approximate Hessians and synchronous transit-guided quasi-Newtonian methods.<sup>46</sup> All saddle points were characterized by means of normal mode analysis, with one imaginary frequency corresponding to rotation of the acetylene ligand. In the case of **Brot** and **Brot'**, additional calculations were performed in order to further confirm that both saddle points correspond to the acetylene rotational process. Displacements in atomic coordinates following the normal mode of the imaginary frequencies were made, and in both species, the subsequent optimization processes led to the reactant and product of the process.

Nuclear magnetic resonance (NMR) properties have been computed by using the gauge-independent atomic orbital (GIAO) method.<sup>38</sup> The bonding situation of the complexes has been analyzed with the help of the NBO partitioning scheme.<sup>47</sup> Furthermore, atomic charges have been calculated by means of the natural population analysis (NPA) method.<sup>47</sup> The topological properties of the electron density<sup>39</sup> were investigated using the XAIM 1.0 program.<sup>48</sup>

**Acknowledgment.** We acknowledge financial support from the DGES of Spain (Projects PB98-1591 and PB98-0916-C02-01, Programa de Promoción General del Conocimiento). The use of the computational facilities of the Centre de Supercomputació i Comunicacions de Catalunya is gratefully appreciated as well.

**Supporting Information Available:** Tables of atomic coordinates and equivalent isotropic displacement coefficients, anisotropic thermal parameters, experimental details of the X-ray studies, and bond distances and angles for **1a** and **2a**. This material is available free of charge via the Internet at <http://pubs.acs.org>.

OM010645N

(42) (a) Parr, R. G.; Yang, W. *Density Functional Theory of Atoms and Molecules*; Oxford University Press: Oxford, U.K., 1989. (b) Ziegler, T. *Chem. Rev.* **1991**, *91*, 651.

(43) (a) Lee, C.; Yang, W.; Parr, R. G. *Phys. Rev. B* **1988**, *37*, 785. (b) Becke, A. D. *J. Chem. Phys.* **1993**, *98*, 5648. (c) Stephens, P. J.; Devlin, F. J.; Chabalowski, C. F.; Frisch, M. J. *J. Phys. Chem.* **1994**, *98*, 11623.

(44) Hay, P. J.; Wadt, W. R. *J. Chem. Phys.* **1985**, *82*, 299. (45) (a) Francl, M. M.; Pietro, W. J.; Hehre, W. J.; Binkley, J. S.; Gordon, M. S.; Defrees, D. J.; Pople, J. A. *J. Chem. Phys.* **1982**, *77*, 3654. (b) Hehre, W. J.; Ditchfield, R.; Pople, J. A. *J. Chem. Phys.* **1972**, *56*, 2257. (c) Hariharan, P. C.; Pople, J. A. *Theor. Chim. Acta* **1973**, *28*, 213.

(46) Peng, C.; Ayala, P. Y.; Schlegel, H. B.; Frisch, M. J. *J. Comput. Chem.* **1996**, *17*, 49.

(47) Reed, A. E.; Curtiss, L. A.; Weinhold, F. *Chem. Rev.* **1988**, *88*, 899.

(48) This program was developed by Jose Carlos Ortiz and Carles Bo, Universitat Rovira i Virgili, Tarragona, Spain.